

# T1 Estimation for Aqueous Iron Oxide Nanoparticle Suspensions Using a Variable Flip Angle SWIFT Sequence

Luning Wang<sup>1</sup>, Curtis Corum<sup>2</sup>, Djaudat Idiyatullin<sup>2</sup>, Michael Garwood<sup>2</sup>, and Qun Zhao<sup>1</sup>

<sup>1</sup>Department of Physics and Astronomy, University of Georgia, Athens, GA, United States, <sup>2</sup>Department of Radiology, University of Minnesota, Minneapolis, MN, United States

**Introduction:** Recently studies demonstrated that Super-paramagnetic iron oxide (SPIO) nanoparticles could be applied to detection and hyperthermia treatment of cancers and cell tracking [1,2]. Quantification of SPIO nanoparticles is usually accomplished by  $T_2^*$  mapping or quantitative susceptibility mapping (QSM) using a gradient-recalled echo (GRE) sequence. However, as the SPIO concentration increases, MR signal loss and image distortions pose serious obstacles to accurately estimate the concentration of SPIO nanoparticles. The SWEEP Imaging with Fourier Transformation (SWIFT) sequence has been designed to minimize short  $T_2^*$  signal loss caused by SPIO nanoparticles [3,4]. Recently Chamberlain et al. [5] proposed a Look-Locker saturation recovery method integrated with the SWIFT to measure  $T_1$ . The SWIFT sequence uses a low flip angle frequency-modulated hyperbolic secant pulse in an inherently spoiled steady state, provides the opportunity to derive a  $T_1$  map through measurements conducted with variable flip angles (VFA). The main problem of VFA methods is ambiguity of the solution in presence of radiofrequency field ( $B_1$ ) inhomogeneities. To overcome this difficulty, we utilize a birdcage coil that provides better  $B_1$  field homogeneity than a surface coil. In addition, for accuracy we use a scheme of small step-size, multiple flip angles. In this work, we propose to utilize the VFA-SWIFT sequence to measure  $T_1$  of ferrofluids with iron concentrations from 0.65 to 6.48 mM/mL. As a comparison,  $T_1$  values were also quantified using the GRE and inversion recovery fast spin echo (IR-FSE) sequence.

**Theory:** For the SWIFT sequence, the magnetic field variation resulting from the applied gradient field is generally large compared to other potential contributions, such as magnetic field inhomogeneity and magnetic susceptibility differences, so their effects are minimal in acquired images. Additionally, SWIFT images are minimally influenced by transverse relaxation, since the dead time between signal excitation and acquisition is usually much shorter than  $T_2^*$  values. Under these circumstances, a region of interest (ROI) in a SWIFT image is immune to signal loss due to  $T_2^*$  values of the scanned subject [6] if signal pile up artifacts are included in the ROI. This leads to  $T_2^*$  independent signal intensity for the ROI in the following form:  $s = M_0 \sin(\alpha) (1 - E_1^{SWIFT}) / (1 - E_1^{SWIFT} \cos(\alpha))$  [3,4]. Therefore, with a fixed repetition time ( $TR$ ), a  $T_1$  estimate can be obtained according to  $[s(\alpha)/\sin(\alpha)] = E_1^{SWIFT} [s(0)/\tan(\alpha)] + M_0(1 - E_1^{SWIFT})$ , where the slope  $E_1^{SWIFT}$  can be numerically solved through a linear least-square fit.  $T_1$  can then be estimated from the natural logarithm of  $E_1^{SWIFT}$  [7].

**Methods:** A SPIO phantom was made of 11 vials with different iron concentrations (see Table 1). The MR experiment was performed on a 7 Tesla Varian Magnex small animal scanner (Agilent Technologies, Santa Clara, CA) that provides a maximum gradient strength of 600mT/m. The phantom was vertically placed in the center of a 7.2 cm transmit/receive birdcage coil. 3D radial SWIFT images were acquired with bandwidth=62.5 kHz,  $TR=8$  ms,  $FOV=80^3$  mm<sup>3</sup>, 32,000 spokes, matrix=256<sup>3</sup>,  $\alpha = 10^\circ, 12^\circ, 16^\circ, 18^\circ, 20^\circ, 24^\circ, 28^\circ$ , and  $32^\circ$ . Additionally, 2D GRE steady state scans were performed with the following parameters:  $TE/TR=2.75/37$  ms, bandwidth=50 kHz,  $FOV=80^2$  mm<sup>2</sup>, matrix=128<sup>2</sup>, average=8, one coronal slice, and the flip angles were varied from  $10^\circ$  to  $32^\circ$  with a step size of  $2^\circ$ . The IR-FSE experiment utilized ETL=8, effective  $TE=8.92$ ms,  $TR=4$ s,  $FOV=80^2$ mm<sup>2</sup>, matrix size = 128<sup>2</sup>, average = 1, one coronal slice,  $TI=100\text{--}1600$ ms with a step size of 100ms. Here, the shortest  $TE$  achievable for the 7T scanner (given the matrix size and FOV) were selected to minimize signal loss caused by the  $T_2^*$  decay for both GRE and IR-FSE scans. A binary mask was created to remove signals outside the phantom on the  $T_1$  maps.

**Results:** Figs. 1(a) and 1(b) display the magnitude images acquired using SWIFT and GRE sequences with  $10^\circ$  flip angle. Fig. 1(c) shows the IR\_FSE image with  $TI$  equal to 800 ms. Vials with different iron concentrations were labeled in Fig. 1(a). The vials with higher concentrations of SPIO nanoparticles appeared brighter than those with lower concentrations. Line-broadening artifacts become more apparent as the concentration increases beyond 4.54 mM (vials 8~11) in Fig. 1(a). For the GRE image, when the vials contains more than 2.59 mM iron (vial 5~11),  $T_2^*$  decay becomes strong and dominant, resulting in significant signal loss and image distortions. In summary, the SWIFT sequence provided positive contrast for the SPIO nanoparticle solutions, whereas GRE and IR-FSE yielded negative contrast. Figs. 1(d-f) show the estimated  $T_1$  maps resulting from the (a) SWIFT, (b) GRE and (c) IR-FSE acquisitions. According to the figure, both SWIFT and GRE sequences resulted in a good  $T_1$  estimation when concentrations were lower than 3.89 mM (vial 1-6).  $T_1$  of ferrofluid in vials 8~11 could only be obtained from Fig. 1(a). The IR-FSE failed to estimate  $T_1$  of vials 2~11. This indicates that the SWIFT sequence is more suitable for measuring  $T_1$  of ferrofluid at high concentrations. As seen from the  $T_1$  maps,  $T_1$  was decreased and the line-broadening artifacts become significant, along with the increase of concentrations.

Fig. 2 (a) and (b) present linear fitting of the relaxation rate  $R_1$  to the various iron concentrations for the SWIFT and GRE sequences. According to the fit, the specific relaxivity ( $r_1$ ) of the ferrofluid was  $0.907 \text{ s}^{-1} \cdot \text{mM}^{-1}$  using the SWIFT method under 7 Tesla. In Fig. 2(b) by using the first seven data points, the resulting relaxivity was equal to  $1.042 \text{ s}^{-1} \cdot \text{mM}^{-1}$ , close to the SWIFT result. The  $R^2$  values for both fittings approximated to 0.95. However, for the GRE result in the Fig. 2(b), standard deviations of the estimated  $R_1$  increased significantly along with the increase of concentrations.

Table 1 summarizes the quantitative  $T_1$  estimates for the various iron concentrations using the SWIFT, GRE and IR-FSE methods. The first two columns list the vial numbers and their iron concentrations, while the estimated  $T_1$  are given in the last three columns. Note that only SWIFT can estimate  $T_1$  for all the concentrations. Additionally, in the presence of high concentrations, standard deviations of the  $T_1$  values measured by SWIFT are still relatively small. The highest concentration at which the GRE method can still measure  $T_1$  is about 3.24 mM, but with a large standard deviation.

**Conclusions:** A VFA-SWIFT sequence was implemented to quantify  $T_1$  of SPIO nanoparticle solutions, compared with the GRE sequence. While the GRE and IR-FSE sequences failed to estimate the  $T_1$  at high iron concentrations, the VFA-SWIFT presented a good linear relationship between the relaxation rate  $R_1$  and iron concentrations, with a relaxivity of approximately  $0.907 \text{ s}^{-1} \cdot \text{mM}^{-1}$  at 7 Tesla.

**Acknowledgements:** The research was funded by grants NIH P41RR008079, P41EB015894, R21CA139688, KL2RR033182, and S10RR023706. In addition we thank Brian Hanna and Michael Tesch for continued collaboration in development of the SWIFT package.

**References:** [1] Richards J.M. et al. Circulation Cardiovascular imaging 2012;5(4):509-517. [2] Zhao Q. et al. Theranostics 2012;2:113-121. [3] Idiyatullin D. et al. J Magn Reson 2006;181(2):342-349 [4] Idiyatullin D. et al. J Magn Reson 2008;193(2):267-273. [5] Chamberlain R. et al. ISMRM proceeding, 2012. [6] Zhou R. et al. Magnetic Resonance in Medicine 2010;63(5):1154-1161. [7] Treier R. et al. Magnetic resonance in medicine 2007;57(3):568-576.

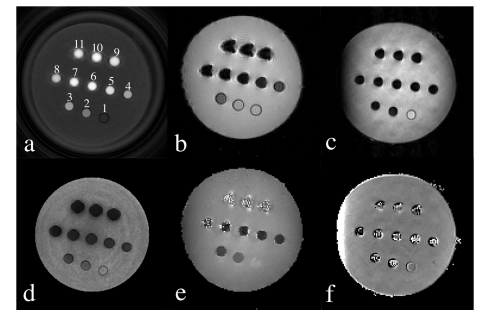


Figure 1. (a) SWIFT and (b) GRE images ( $\alpha=10^\circ$ ) and (c) IR-FSE ( $TI=800$ ms) are illustrated in the first row. Vials are labeled from 1 to 11 based on their concentrations from low to high.  $T_1$  maps in the second row were estimated by using the (d) SWIFT, (e) GRE, and (f) IR-FSE datasets.

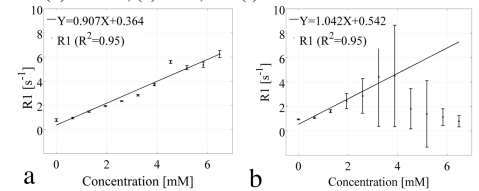


Figure 2. Concentrations of the different vials are linearly fitted to their  $R_1$  values estimated by the (a) SWIFT and (b) GRE (without the last four data points) based methods.

Vial	Iron	SWIFT	GRE	IR-FSE
1	0	1358 ± 251	1064 ± 41	952 ± 655
2	0.65	1092 ± 95	929 ± 48	729 ± 239
3	1.30	679 ± 34	622 ± 50	–
4	1.94	519 ± 15	426 ± 77	–
5	2.59	431 ± 9	391 ± 106	–
6	3.24	357 ± 8	299 ± 116	–
7	3.89	275 ± 7	–	–
8	4.54	181 ± 5	–	–
9	5.18	201 ± 9	–	–
10	5.83	192 ± 8	–	–
11	6.48	165 ± 9	–	–

Table 1. Iron concentrations (in mM/mL) of the different vials are listed in the second column. The  $T_1$  values (in [ms]) estimated by the SWIFT, GRE and IR-FSE based methods are presented in the last three columns.